ORIGINAL RESEARCH

The Combined Effects of Circular RNA Methylation Promote Pulmonary Fibrosis

Sha Wang[1,2,3,4*], Wei Luo[1,2,3,4*], Jie Huang[1,2], Mengling Chen[1,4], Jiawei Ding[1,4], Yusi Cheng[1], Wei Zhang[1,4], Shencun Fang[1], Jing Wang[1,2‡], and Jie Chao[1,2,3,4,5‡]

[1]Department of Physiology, School of Medicine, Southeast University, Nanjing, Jiangsu, China; [2]Jiangsu Provincial Key Laboratory of Critical Care Medicine, Zhongda Hospital, School of Medicine, Southeast University, Nanjing, Jiangsu, China; [3]Key Laboratory of Environmental Medicine Engineering, Ministry of Education, School of Public Health, and [4]Key Laboratory of Development Genes and Human Disease, Southeast University, Nanjing, Jiangsu, China; and [5]School of Medicine, Xizang Minzu University, Xianyang, Shanxi, China

ORCID ID: 0000-0002-7800-3557 (J.C.).

Abstract

m^{6}A (N^6-methyladenosine) is the most common type of RNA methylation modification, mainly occurring on mRNA. Whether m^{6}A-modified circular RNAs (circRNAs) are involved in pulmonary fibrosis in different settings remains unclear. Using an m^{6}A–circRNA epitranscriptomic chip, candidate circRNAs were selected, among which hsa_circ_0000672 and hsa_circ_0005654 were specifically involved in SiO_2-induced pulmonary fibrosis by targeting the same protein, eIF4A3, indicating that the m^{6}A modification of these two circRNAs has a synergistic effect on fibroblast dysfunction induced by SiO_2. A mechanistic study revealed that the m^{6}A modification of circRNAs was mainly mediated by the methyltransferase METTL3. Furthermore, METTL3 promoted the activation, migration, and activity of pulmonary fibroblasts and participated in SiO_2-induced pulmonary fibrosis via the circRNA m^{6}A modification. m^{6}A methylation of circRNAs mediates silica-induced fibrosis, enriching the understanding of circRNAs and uncovering a potential new target for treating fibrosis-related diseases.

Keywords: noncoding RNA; m^{6}A; pulmonary fibrosis; METTL3

Silicosis, the most common type of pneumoconiosis, is a pulmonary fibrosis disease caused by the long-term inhalation of large amounts of free silica (1). Inhaled silica particles can reach and persist in the peripheral lung (2). After being engulfed by alveolar macrophages (AMs), SiO_2 triggers a series of inflammatory reactions, followed by fibrosis (3). The greatest challenges in silicosis diagnosis and treatment include the lack of a clear diagnostic target in the early stage and lack of effective treatment measures in the late stage. Although the role of SiO_2-induced chemokines and cytokines released from AMs has been extensively studied, recent studies have suggested that the direct effect of SiO_2 on fibroblasts also plays an important role in the pathogenesis of fibrosis (4, 5). Therefore, exploring the pathogenesis of silicosis and identifying early diagnostic targets and late treatment measures are critical. Circular RNAs (circRNAs) are a class of closed circular noncoding RNAs formed after trans-splicing.

(Received in original form August 26, 2021; accepted in final form January 21, 2022)

*These authors contributed equally to this work.

‡Co–senior authors.

Supported by resources and facilities at the Core Laboratory at the Medical School of Southeast University, the National Key R&D Program of China (2017YFA0104303), and the National Natural Science Foundation of China (81972987, 81773796, 81700068, and 81803182).

Author Contributions: S.W. and W.L. performed the experiments, interpreted the data, prepared the figures, and wrote the manuscript. J.H, M.C., J.D., Y.C., W.Z., and S.F. performed the experiments and interpreted the data. J.W. designed the experiments, interpreted the data, and wrote the manuscript. J.C. provided laboratory space and funding, designed the experiments, interpreted the data, wrote the manuscript, and directed the project. All of the authors read, discussed, and approved the final manuscript.

All of the relevant raw data and materials are freely available to any scientist upon request.

Correspondence and requests for reprints should be addressed to Jie Chao, Ph.D., Department of Physiology, School of Medicine, Southeast University, 87 Dingjiaqiao Road, Nanjing, Jiangsu, 210009, China. E-mail: chaojie@seu.edu.cn.

This article has a related editorial.

This article has a data supplement, which is accessible from this issue's table of contents at www.atsjournals.org.

Am J Respir Cell Mol Biol Vol 66, Iss 5, pp 510–523, May 2022

Originally Published in Press as DOI: 10.1165/rcmb.2021-0379OC on February 25, 2022
Internet address: www.atsjournals.org

Because of the lack of 5′ or 3′ ends, they are relatively stable and can generally resist exonuclease degradation (6). In recent years, the study of RNA epigenetics has become a popular approach in various fields, and RNA m^6A (N^6-methyladenosine) modification, the most abundant RNA modification in eukaryotes, has become a new research hotspot. m^6A modification is the most common post-transcriptional modification of RNA in the transcriptome (7). m^6A modification involves the attachment of a methyl group to the sixth nitrogen atom of adenine. m^6A modification is also a dynamic process, including methylation and demethylation. Similar to the DNA methylation process, RNA m^6A modification is catalyzed by methyltransferases and demethylases. Methyltransferases ("writers") mainly include METTL3, METTL14, WTAP, KIAA1429, RBM15, and ZC3H13, whereas demethylases ("erasers") mainly include FTO and ALKBH5. In addition, readers, including YTHDF1, YTHDF2, and YTHDF3, recognize m^6A-modified RNA and then perform functions (8). Studies have shown that m^6A modification can regulate the stability, transport, splicing, and translation of RNA at the molecular level (9, 10), and circRNAs also have various biological functions and are involved in the pathogenesis of Alzheimer's disease, rectal cancer, depression, ischemia/reperfusion injury and other diseases (11–16). Recent studies have shown that m^6A-modified circRNAs can mediate resistance to sorafenib by regulating β-catenin signaling in hepatocellular carcinoma (17). Although a relationship between m^6A and certain tumors has been found in recent years, the mechanism of m^6A modification in pulmonary fibrosis is unclear. The current study mainly focused on the initiation of fibrosis, and the time point of interest was during the early stage of silicosis (7 d). Although methylation shows a rapid and transient increase pattern in fibroblasts *in vitro*, whether methylation remains high in an *in vivo* setting deserves further investigation, as fibrosis may be because of fibroblast proliferation, endothelial mesenchymal transformation, or epithelial mesenchymal transformation (18–20).

In this study, we investigated the role of m^6A modification in pulmonary fibrosis, demonstrated the role of m^6A-modified circRNAs in silicosis fibrosis, revealed a new regulatory model of circRNAs in silicosis, provided evidence of the correlation between m^6A-modified circRNAs and disease, and enriched theoretical research on circRNAs.

Some of the results of these studies have been previously reported in preprint form (https://doi.org/10.1101/2021.08.05.455186).

Methods

Reagents

SiO_2 particles with diameters of approximately 1–5 μm were purchased from Sigma–Aldrich. Primary antibodies against METTL3, METTL14, WTAP, ALKBH5, FTO, ACTA2 (α-SMA), and FN1 were purchased from Proteintech. Antibodies against COL1A2 and GAPDH (MB001, mouse) were obtained from Bioworld, Inc. Antibodies against eIF4A3 were obtained from Affinity. Antibodies against p-PYK2 were obtained from ABCAM.

Measurement of Total m^6A

The m^6A concentrations of total RNA were measured using an EpiQuik m^6A RNA Methylation Quantification Kit (Colorimetric; Epigentek) following the manufacturer's protocol. Total RNA was isolated from HPF-a cells and lung tissue using the TRIzol reagent. In total, 200 ng of RNA was required for each sample.

m^6A RNA IP

m^6A RNA IP (RIP) was performed using the Magna RIP Kit according to the manufacturer's instructions. Briefly, the cells were collected, and the same volume of RIP lysate was added to lyse the cells. The cells were placed on ice for 5 minutes, and the cells were completely lysed overnight at −80°C. The supernatant was centrifuged the following day. Next, magnetic beads were prepared for IP. The anti-m^6A antibody and mouse IgG were incubated with the magnetic beads in buffer at room temperature for 30 minutes, and the cell lysate supernatant was mixed with the magnetic bead-antibody complex and incubated overnight at 4°C. The circRNA containing the m^6A site was eluted on the second day, and the immunoprecipitated RNA was purified and extracted using phenol–chloroform-isoamyl alcohol. The extracted RNA was measured using the Nanodrop system for reverse transcription, followed by real-time PCR.

Arraystar m^6A-circRNA Epitranscriptomic Chip High-Throughput Assay

The mouse model of silicosis was established according to the above method. The lung tissues of mice in the control group and model group were collected, and a high-throughput Arraystar m^6A-circRNA Epitranscriptomic chip was used by Shanghai Kangcheng Biotech to investigate the differential m^6A modification of circRNA in the lung tissues of mice in the control and model groups. The m^6A methylation for a transcript was calculated as the percentage of modified RNA in all RNAs based on the IP (Cy5-labeled) and supernatant (Cy3-labeled) normalized intensities. The "m^6A quantity" was calculated for the m^6A methylation amount of each transcript based on the IP (Cy5-labeled) normalized intensities.

Statistical Analysis

GraphPad Prism 8.0.1 was used for statistical analysis, and all data are expressed as the mean ± SD. A *t* test was used for comparisons between two groups, two-way ANOVA was used for comparisons between multiple groups, and significance was considered at a P value of less than 0.05.

Results

m^6A-modified circRNAs in the Lung Tissue of Silicosis Model Mice

The degree of m^6A modification in circRNAs was detected by constructing a mouse model of silicosis. First, an Arraystar m^6A-circRNA Epitranscriptomic microarray was used to investigate the differences in m^6A modification in circRNAs in the lung tissues of mice in the silicosis (7 d) and control groups (Figure 1A). Differences were found in the relative degree of m^6A-modified circRNAs and the relative quantity of m^6A-modified circRNAs in the lung tissues of mice in the control and silicosis groups (Figures 1B–1E). Among them, 24 were upregulated and 674 were downregulated in the relative degree of m^6A-modified circRNAs, whereas 132 were upregulated and 336 were downregulated, in the relative quantity of m^6A-modified circRNAs. These results indicated that the differences in m^6A modification in circRNAs might be involved in the pathological process in the lung after exposure to SiO_2.

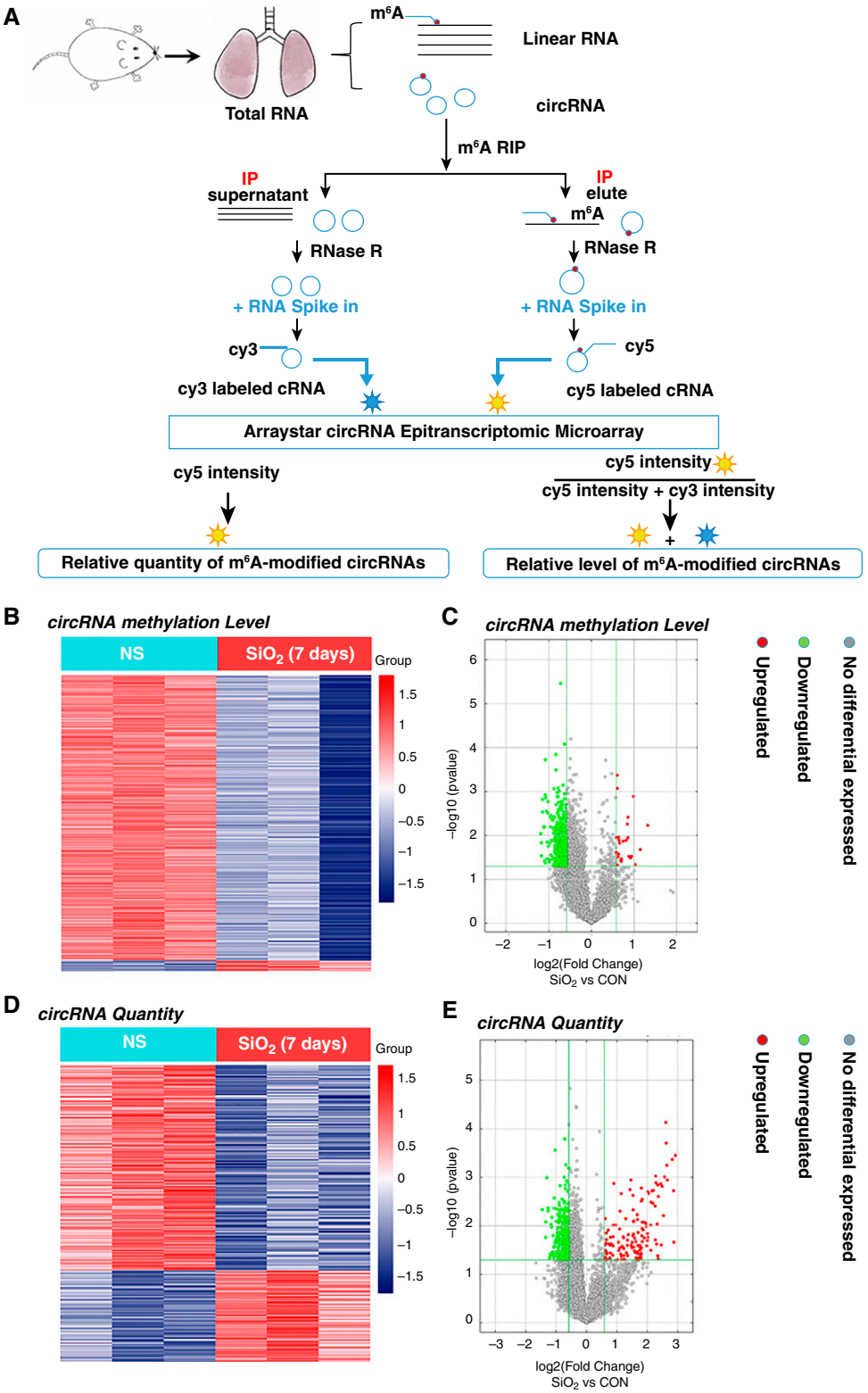

Figure 1. m^{6}A (N^6-methyladenosine) modification of circular RNAs (circRNAs) in silicosis. (*A*) Arraystar m^{6}A-circRNA epitranscriptomic microarray flow. (*B*) The heatmap shows the difference in the concentrations of m^{6}A-modified circRNAs, and the red and blue strips indicate increased and decreased m^{6}A concentrations, respectively ($n = 3$). (*C*) The volcano map shows the difference in the concentration of m^{6}A-modified circRNAs. (*D*) Heatmap showing the difference in the quantity of m^{6}A-modified circRNAs. The red and blue strips indicate circRNAs with upregulated and downregulated expression, respectively ($n = 3$). (*E*) The volcano map shows the difference in the quantity of m^{6}A-modified circRNAs. con = control; NS = normal saline; RIP = RNA immunoprecipitation.

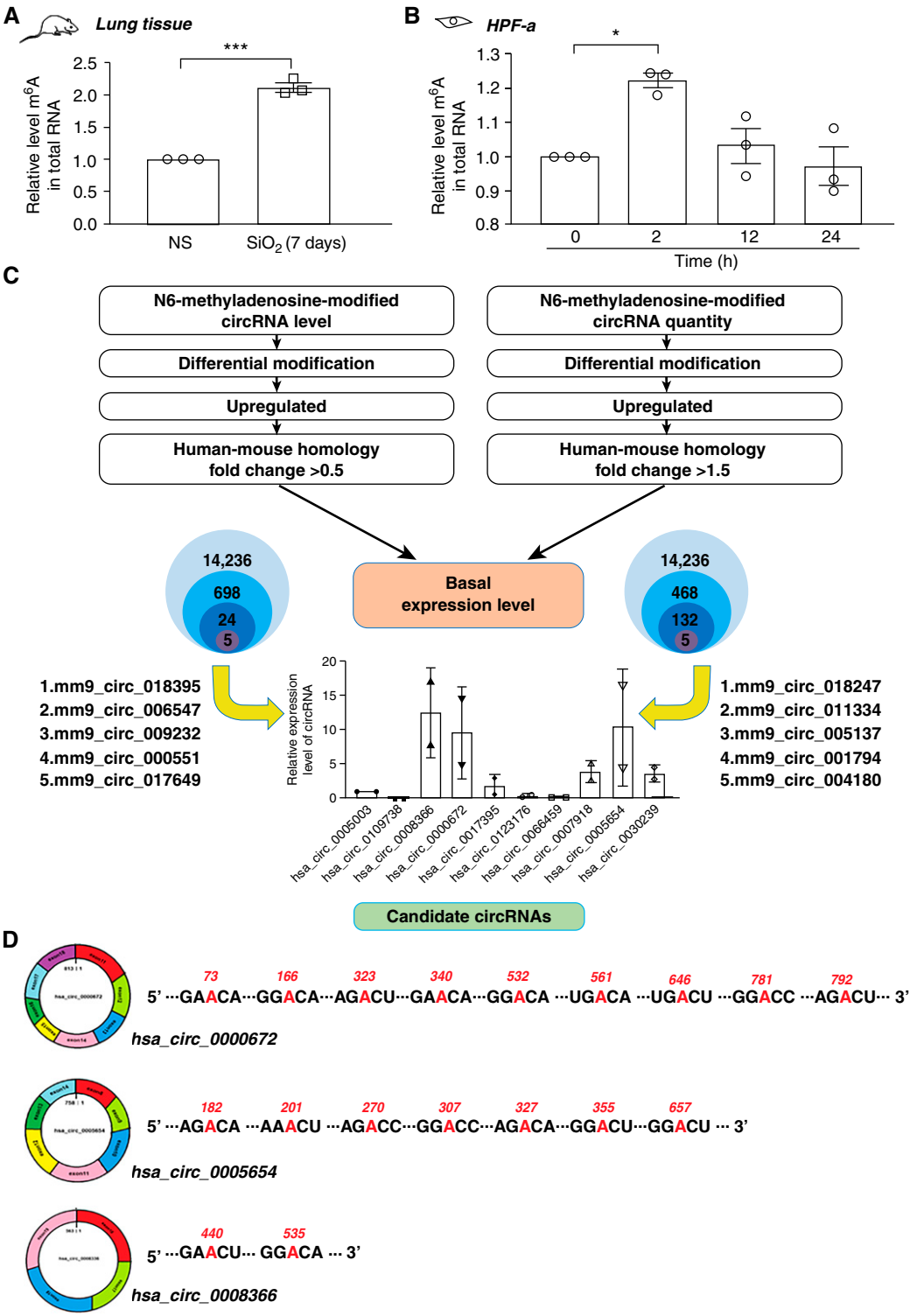

Figure 2. Preliminary screening of circRNAs. (*A*) The total RNA m^{6}A concentration in the lung tissues of mice was detected using the EpiQuik m^{6}A RNA Methylation Quantification Kit. The data are presented as the mean ± SD, $n = 3$. ***$P < 0.001$. (*B*) The EpiQuik m^{6}A RNA Methylation Quantification Kit detects total RNA m^{6}A concentrations in human pulmonary fibroblasts treated with SiO_2 for different periods. The data are presented as the mean ± SD, $n = 3$. *$P < 0.05$. (*C*) Screening process of circRNAs; the basic degrees of expression of 10 circRNAs in human pulmonary fibroblasts were detected by PCR; the data are presented as the mean ± SD, $n = 2$. (*D*) Analysis of three circRNA m^{6}A sites.

Table 1. Candidate circRNAs Homologous to Humans and Mice

mm9 circRNA	Conserved hsa circRNA	hsa circRNA Parental Gene	Genomic Length (bp)	Spliced Seq Length (bp)	Number of m^6A Sites
mm9_circ_018395	has_circ_0123176	ACAP2	24,617	572	6
mm9_circ_006547	hsa_circ_0005654	PRDM5	56,897	758	7
mm9_circ_009232	hsa_circ_0008336	BBS9	30,390	563	2
mm9_circ_000551	hsa_circ_0109738	DACT3	416	250	3
mm9_circ_017649	hsa_circ_0005003	AGAP1	9,526	363	1
mm9_circ_018247	hsa_circ_0066459	MAGI1	15,040	327	9
mm9_circ_011334	hsa_circ_0007918	SLC2A13	19,910	369	3
mm9_circ_005137	hsa_circ_0030239	FNDC3A	69,213	214	1
mm9_circ_001794	hsa_circ_0017359	ZMYND11	30,055	295	4
mm9_circ_004180	hsa_circ_0000672	CLEC16A	40,830	813	9

Definition of abbreviations: bp = base pair; circRNA = circular RNA; m^6A = N^6-methyladenosine; Seq = sequence.

Preliminary Screening of circRNAs

To further understand the correlation of the degree of m^6A modification between circRNA and total RNA, both the lung tissue of mice and human pulmonary fibroblasts treated with SiO_2 were collected for detection of the total degree of RNA m^6A modification. The m^6A concentration in the lung tissue of the silicosis group was significantly higher than that in the control group by approximately twofold (Figure 2A), and the degree of m^6A modification of total RNA in the human pulmonary fibroblasts treated with SiO_2 increased sharply at 2 hours and then returned to normal amounts (Figure 2B), indicating that m^6A modification occurred in the pulmonary fibroblasts and might be involved in pulmonary fibrosis. Preliminary screening of circRNAs with increased amounts of m^6A modification was conducted because of upregulation of m^6A modification in both lung tissue and cultured fibroblasts, in which 10 circRNAs homologous in humans and mice (circBase [http://www.circbase.org/] and circbank [http://www.circbank.cn/] databases) (Table 1) with the most increased degrees of m^6A modification were selected (Figure 2C). Next, the degrees of basic expression of the 10 circRNAs were detected, three of which had high degrees of expression (Figure 1C). The predicted m^6A sites (SRAMP database [http://www.cuilab.cn/sramp]) of the three circRNAs are shown. All three screened circRNAs had more than one m^6A site. Among them, hsa_circ_0000672 and hsa_circ_0005654 had nine and seven m^6A sites, respectively, whereas hsa_circ_0008336 had two m^6A sites, hsa_circ_0000672 and hsa_circ_0005654 comprised eight and seven exons, respectively, and hsa_circ_0005654 comprised four exons (Figure 2D and Figure E1 in the data supplement). These three candidate circRNAs were selected for further investigation.

hsa_circ_0000672 and hsa_circ_0000672 Are Involved in SiO_2-induced Fibroblast Dysfunction

To determine the role of candidate circRNAs, siRNA was applied to knock down their expression (Figure E2A). First, the effects of these three circRNAs on the activation of human pulmonary fibroblasts were detected, as indicated by changes in the fibroblast activation markers FN1, Collagen 1, and ACTA2. The knockdown of hsa_circ_0000672, hsa_circ_0005654 (Figures E2B–E2E) and hsa_circ_0008336 (Figures E2F–E2I) alone did not affect the SiO_2-induced upregulation of FN1, Collagen 1, and ACTA2. Furthermore, knockdown of these three circRNAs alone did not affect cell migration (Figures E3A and E3B). Considering the relatively low expression of most circRNAs (21), whether multiple circRNAs work together deserves to be investigated. Therefore, simultaneous knockdown of different combinations of candidate circRNAs was performed. Surprisingly, only the simultaneous knockdown of hsa_circ_0000672 and hsa_circ_0005654 abolished fibroblast activation induced by SiO_2 (Figures 3A–3D). Similarly, cell migration induced by SiO_2 was significantly inhibited after the knockdown of these two circRNAs (Figures 3E and 3F). Moreover, hsa_circ_0000672 and hsa_circ_0005654 knockdown together abolished fibroblast activation induced by SiO_2 in the MRC-5 cell line (Figures 3G and 3H). Taken together, the cooperation of hsa_circ_0000672 and hsa_circ_0005654 might be involved in SiO_2-induced fibroblast dysfunction.

eIF4A3 Is Involved in SiO_2-induced Fibroblast Dysfunction

We speculated why these two circRNAs are required for fibroblast dysfunction simultaneously. First, to confirm the existence of these two circRNAs, divergent and convergent primers to amplify hsa_circ_0000672 and hsa_circ_0005654 circular transcripts and linear transcripts were applied, respectively. PCR showed that hsa_circ_0000672 and hsa_circ_0005654 were detected only in cDNA but not in genomic DNA (gDNA) using divergent primers. Linear transcripts were amplified from both cDNA and gDNA using convergent primers (Figures E4A and E4B), indicating the existence of circRNAs in fibroblasts. As expected, SiO_2 treatment did not change the expression of the two circRNAs (Figure 4A), indicating that epigenetic modification might be the main mode of action for these two circRNAs. Furthermore, *in situ* hybridization experiments demonstrated that hsa_circ_0000672 and hsa_circ_0005654 were mainly located in the cytoplasm of fibroblasts (Figure 4B). Next, to clarify why these two circRNAs show joint-work characteristics, circInteractome (https://circinteractome.nia.nih.gov/index.html) was applied to conduct bioinformatics analysis. A common RNA binding protein (RBP), eIF4A3, was revealed to bind to the flanking intron sequences of these two circRNA pre-mRNAs (Figure 4C).

eIF4A3 is a eukaryotic translation initiation factor that promotes the

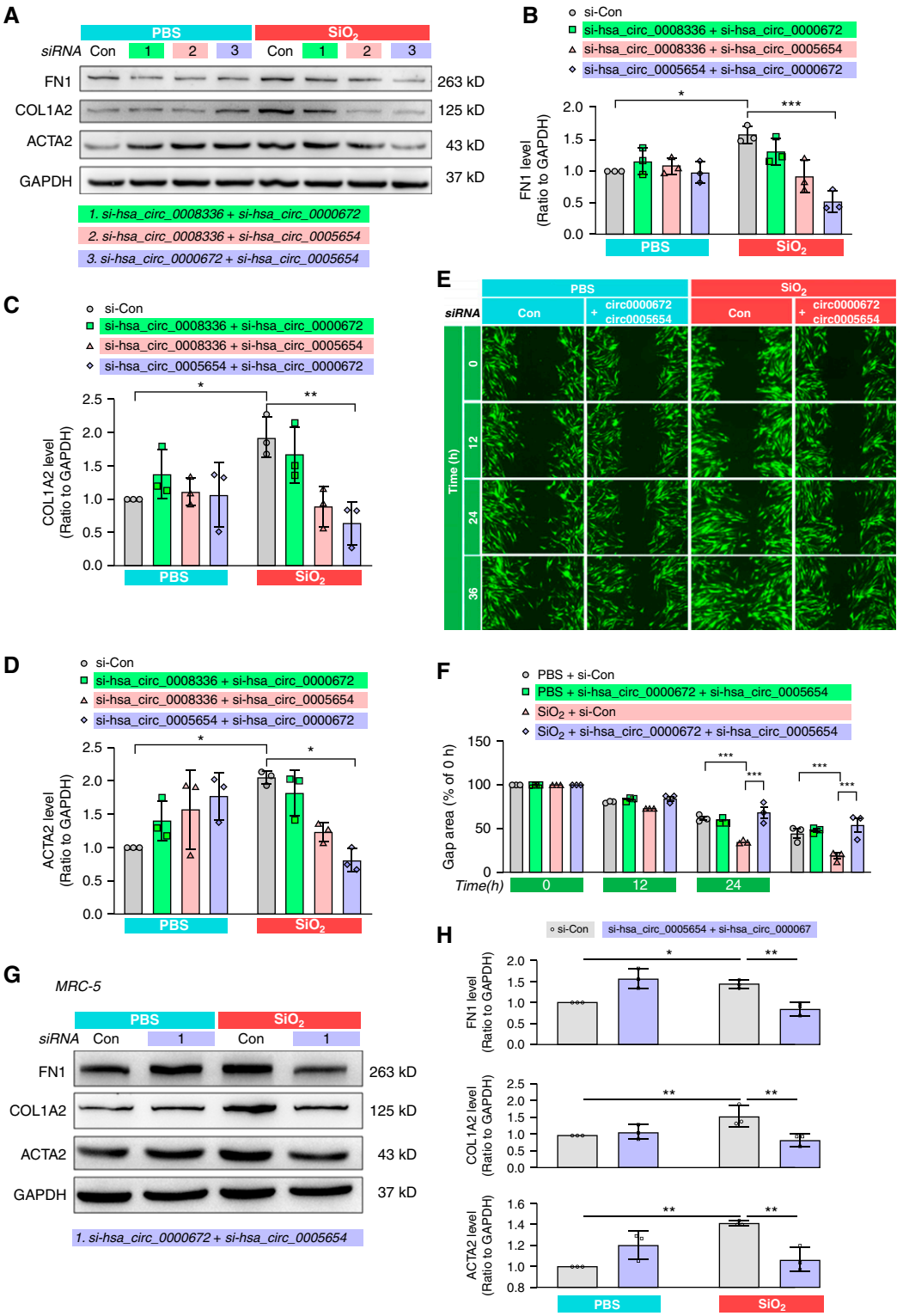

Figure 3. hsa_circ_0000672 and hsa_circ_0005654 promote the activation, migration, and activity of human pulmonary fibroblasts. (*A–D*) WB was used to detect the effects of hsa_circ_0000672 and hsa_circ_0005654 knockdown on the human pulmonary fibroblast activation marker proteins FN1 (fibronectin 1), Collagen 1, and ACTA2. The data are presented as the mean ± SD, $n = 3$. *$P < 0.05$, **$P < 0.01$, and ***$P < 0.001$. (*E* and *F*) The effect of hsa_circ_0000672 and hsa_circ_0005654 knockdown on the migration of human pulmonary fibroblasts was examined using the wound-healing assay. Scale bar, 325 μm. The data are presented as the mean ± SD, $n = 3$. ***$P < 0.001$. (*G* and *H*) Western blot (WB) was used to detect the effects of hsa_circ_0000672 and hsa_circ_0005654 knockdown on the human pulmonary fibroblast activation marker proteins FN1, Collagen 1, and ACTA2 in the MRC-5 cell line. The data are presented as the mean ± SD, $n = 3$. *$P < 0.05$ and **$P < 0.01$.

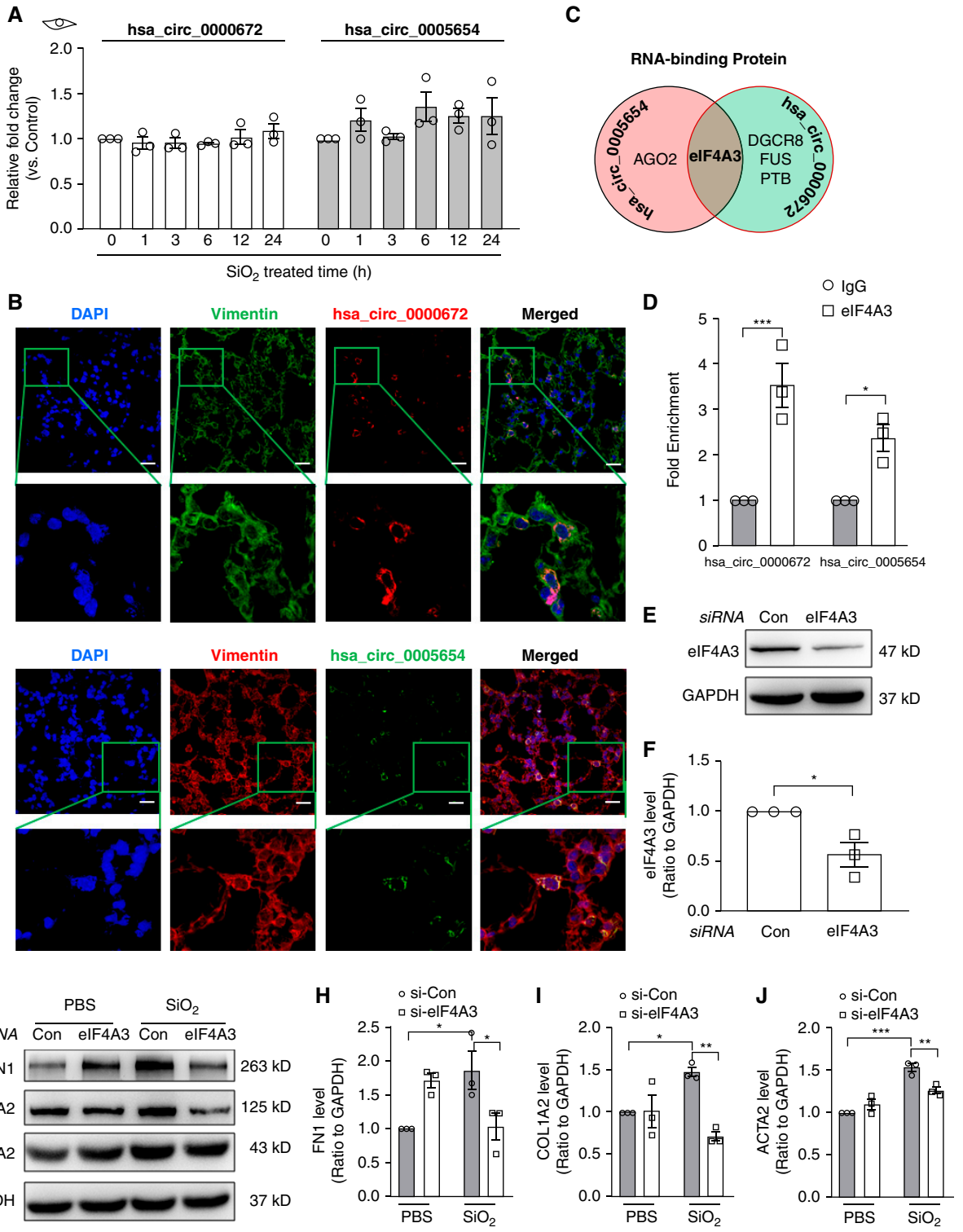

Figure 4. As the target proteins of hsa_circ_0000672 and hsa_circ_0005654, eIF4A3 promotes the activation, migration and activity of human lung fibroblasts. PCR was used to detect the expression of hsa_circ_0000672 and hsa_circ_0005654 in human lung fibroblasts at different time points. The data are presented as the mean ± SD, $n = 3$. (*B*) *In situ* hybridization showed that hsa_circ_0000672 and hsa_circ_0005654 were present in the cytoplasm. Scale bars, 20 μm. (*C*) Bioinformatics analysis showed that hsa_circ_0000672 and hsa_circ_0005654 pre-mRNAs have a common RNA binding protein (RBP). (*D*) The RIP test was used to detect the interaction of hsa_circ_0000672 and hsa_circ_0005654 with eIF4A3. (*E* and *F*) Knockdown efficiency of EIF4A3. The data are presented as the mean ± SD, $n = 3$. *$P < 0.05$. (*G–J*) WB was used to detect the effects of knockdown of eIF4A3 on the human pulmonary fibroblast activation marker proteins FN1, Collagen 1, and ACTA2. The data are presented as the mean ± SD, $n = 3$. *$P < 0.05$, **$P < 0.01$, and ***$P < 0.001$. eIF4A3 = eukaryotic translation initiation factor 4A3.

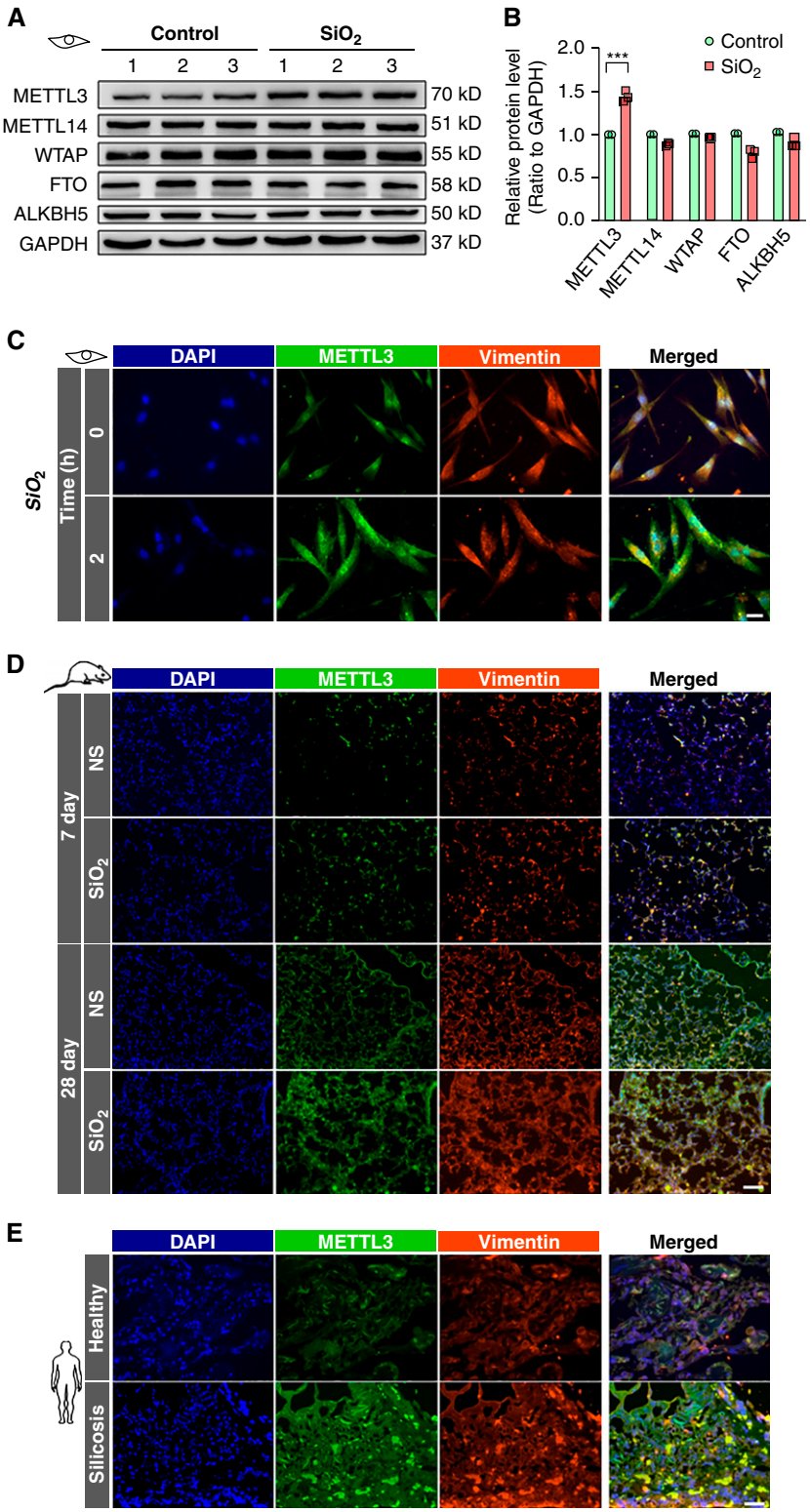

Figure 5. METTL3 expression is elevated in pulmonary fibrosis. (*A* and *B*) WB and quantitative PCR were used to detect changes in the five representative m^6A modification enzymes in pulmonary fibroblasts. The data are presented as the mean ± SD, $n = 3$. ***$P < 0.001$. (*C*) METTL3 expression was detected by cellular immunofluorescence. Scale bar, 30 μm. (*D*) METTL3 expression in the lung tissues of mice at 7 and 28 days after modeling was detected by immunofluorescence. Scale bar, 50 μm. (*E*) METTL3 expression in the lung tissues of healthy individuals and silicosis patients was detected by immunofluorescence. Scale bar, 50 μm. METTL3 = methyltransferse like 3; pPCR = quantitative Real-time PCR.

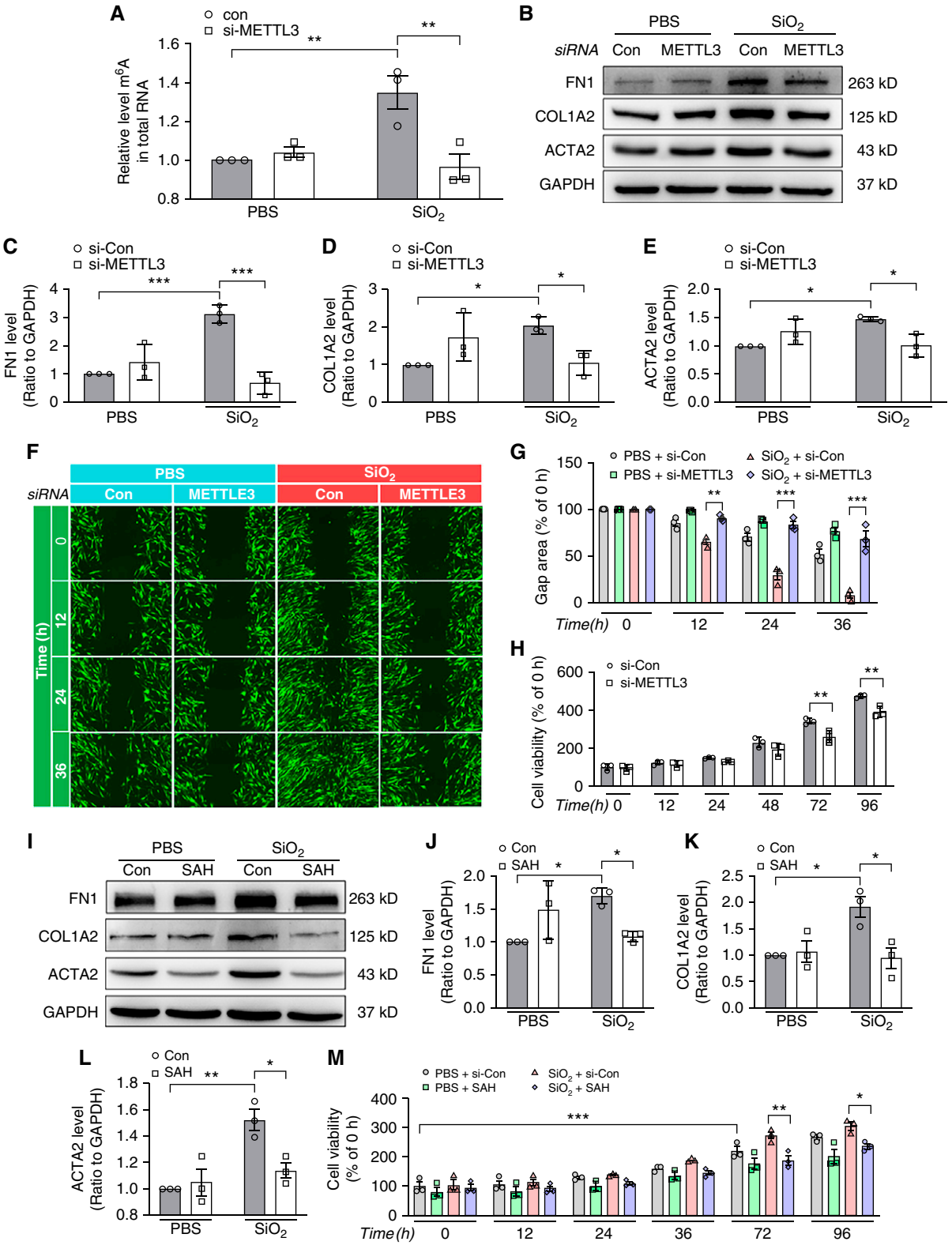

Figure 6. METTL3 mediates RNA m^{6}A modification and promotes the activation, migration, and activity of human pulmonary fibroblasts. (*A*) The EpiQuik m^{6}A RNA Methylation Quantification Kit was used to detect total RNA m^{6}A concentrations in human pulmonary fibroblasts after METTL3 knockdown. The data are presented as the mean ± SD, $n = 3$. $^{**}P < 0.01$. (*B–E*) WB was used to detect the effects of METTL3 knockdown on the human pulmonary fibroblast activation markers FN1, Collagen 1 and ACTA2. The data are presented as the mean ± SD, $n = 3$. $^{*}P < 0.05$ and $^{***}P < 0.001$. (*F* and *G*) The wound-healing assay was used to detect the effect of METTL3 knockdown on the migration of human pulmonary

formation of circRNAs. Studies have found that eIF4A3 binds to MMP9 mRNA transcripts, inducing the cyclization of circMMP9 in glioblastoma multiforme (GBM) and increasing the expression of circMMP9 (22). However, previous results have suggested that the expression of hsa_circ_0000672 and hsa_circ_0005654 did not change with SiO_2 exposure. Thus, the binding of eIF4A3 to the flanking intron sequence of circRNA pre-mRNA might not be a major factor. Therefore, we questioned whether these two circRNAs also interacted with eIF4A3. We verified through RIP experiments in 293T cells that hsa_circ_0000672 and hsa_circ_0005654 could bind to eIF4A3, confirming this hypothesis (Figure 4D). To further understand the role of eIF4A3 in fibroblast dysfunction induced by SiO_2, knockdown of eIF4A3 was performed (Figures 4E and 4F), in which the upregulation of fibroblast markers after SiO_2 exposure was attenuated (Figures 4G–J). The above results indicated that hsa_circ_0000672 and hsa_circ_0005654 synergistically targeted eIF4A3, followed by fibroblast dysfunction.

The Amount of METTL3 Increases *In Vivo* and *In Vitro*

With the elucidation of the effect of two circRNAs, the upstream mechanism of m^6A modification on circRNAs should be clarified. Because m^6A modification involves methyltransferases and demethylases, which depend on the expression of m^6A-modification enzymes, the concentrations of five representative m^6A-modification enzymes were detected after SiO_2 exposure in fibroblasts. Only the degree of expression of METTL3 showed an increase after SiO_2 exposure (Figures 5A, 5B, E5A, and E5B), a finding that was confirmed by immunofluorescence staining (Figure 5C), whereas the other enzymes showed no change. Furthermore, the mRNA concentrations of the five enzymes were not affected by SiO_2 exposure (Figure E5C), indicating that a nontranscriptional regulation mechanism might be involved. To validate the *in vitro* findings, immunofluorescence staining was conducted in the lung tissues of mice and human donors. METTL3 expression was elevated in the pulmonary fibroblasts of mice after 7 and 28 days of SiO_2 exposure (Figure 5C). Consistent with these findings, immunofluorescence staining of lungs from healthy subjects and patients with silicosis also showed elevated METTL3 concentrations in pulmonary fibroblasts (Figure 5E). Taken together, these results indicated that METTL3 might be the main m^6A-modification enzyme in fibroblast dysfunction after SiO_2 stimulation.

METTL3 Mediates RNA m^6A Modification and Is Involved in SiO_2-induced Fibroblast Dysfunction

To further understand the effect of METTL3 on pulmonary fibroblasts, METTL3 siRNA in HPFs was applied (Figures E6A and E6B). Compared with the control group, METTL3 knockdown abolished the upregulation in the total RNA m^6A concentration induced by SiO_2 (Figure 6A), confirming the role of METTL3 in m^6A modification. Furthermore, METTL3 knockdown significantly reduced the induction of fibroblast activation markers (Figures 6B–6E) and fibroblast migration (Figures 6F and 6G). In addition, the phosphorylation of PYK2, a protein related to cell migration and invasion (23, 24), was also attenuated after METTL3 knockdown (Figures E6C and E6D). Consistently, the increase in cell viability induced by SiO_2 was inhibited with METTL3 knockdown (Figure 6H). Moreover, METTL3 knockdown significantly reduced the induction of fibroblast activation markers in MRC-5 cells (Figure 7A-D). To further confirm the role of METTL3 in fibroblast activation, SAH (METTL3-METTL14 heterodimer complex inhibitor) (25) was applied to pretreat fibroblasts for 2 hours. SAH abolished the increase in fibroblast activation markers induced by SiO_2 (Figure 6I-L). Similarly, SAH pretreatment inhibited ascendant fibroblast viability induced by SiO_2 (Figure 6M), a finding that was consistent with the result of METTL3 knockdown. Moreover, METTL3 knockdown significantly reduced the induction of eIF4a3 induced by SiO2 in both HPF-a and MRC-5 cells (Figures E7E–E7H). Collectively, these experiments demonstrated that METTL3 mediates RNA m^6A modification and is involved in SiO_2-induced fibroblast dysfunction.

METTL3 Mediates circRNA m^6A Modification, and m^6A-modified circRNAs Are Involved in SiO_2-induced Fibroblast Dysfunction

The role of circRNAs and METTL3 in fibroblast dysfunction having been proven, whether METTL3 mediates the m^6A modification of circRNAs, as well as the m^6A-modified circRNAs involved in SiO_2-induced fibroblast dysfunction, must be clarified. *In situ* hybridization and immunofluorescence experiments indicated the colocalization of METTL3 with hsa_circ_0000672 and hsa_circ_0005654 (Figures 7A, E8A, and E8B). RIP experiments showed that METTL3 binds with hsa_circ_0000672 and hsa_circ_0005654 (Figure 7B). Furthermore, although METTL3 knockdown did not affect the expression of hsa_circ_0000672 and hsa_circ_0005654 (Figure 7C), METTL3 knockdown significantly reduced the degrees of m^6A modification of circRNAs (Figure 7D), indicating that METTL3 was not involved in the expression of hsa_circ_0000672 and hsa_circ_0005654 but in the m^6A modification of circRNAs.

Furthermore, hsa_circ_0000672 and hsa_circ_0005654 with mutated m^6A sites (Figure 7E) were applied to confirm the connection between m^6A-modified circRNAs and fibroblast function. Hsa_circ_0000672 and hsa_circ_0005654 with the m^6A site mutated or wild-type overexpression plasmids were constructed, respectively. Sequencing results proved that the overexpressed plasmid was successfully constructed and induced overexpression in HPF-a cells (Figures 7F and 7G) and 293T cells (Figures E9A and E9B). We have previously shown that circRNA knockdown significantly reduced the increase in fibroblast activation markers after SiO_2 exposure (Figure 3A-D). Here, to

Figure 6. (*Continued*). fibroblasts. Scale bar, 325 μm. $^{**}P < 0.01$ and $^{***}P < 0.001$. (*H*) The Cell Counting Kit-8 (CCK-8) assay was used to detect the effect of METTL3 knockdown on the activity of human pulmonary fibroblasts. The data are presented as the mean ± SD, $n = 3$. $^{**}P < 0.01$. (*I–L*) WB was used to detect the effects of the *S*-Adenosylhomocysteine (SAH) inhibitor on the fibroblast activation markers FN1, Collagen 1, and ACTA2. The data are presented as the mean ± SD, $n = 3$. $^{*}P < 0.05$. (*M*) The Cell Counting Kit-8 assay was used to detect the effect of the SAH inhibitor on the viability of human pulmonary fibroblasts. The data are presented as the mean ± SD, $n = 3$. $^{*}P < 0.05$, $^{**}P < 0.01$, and $^{***}P < 0.001$. con = control.

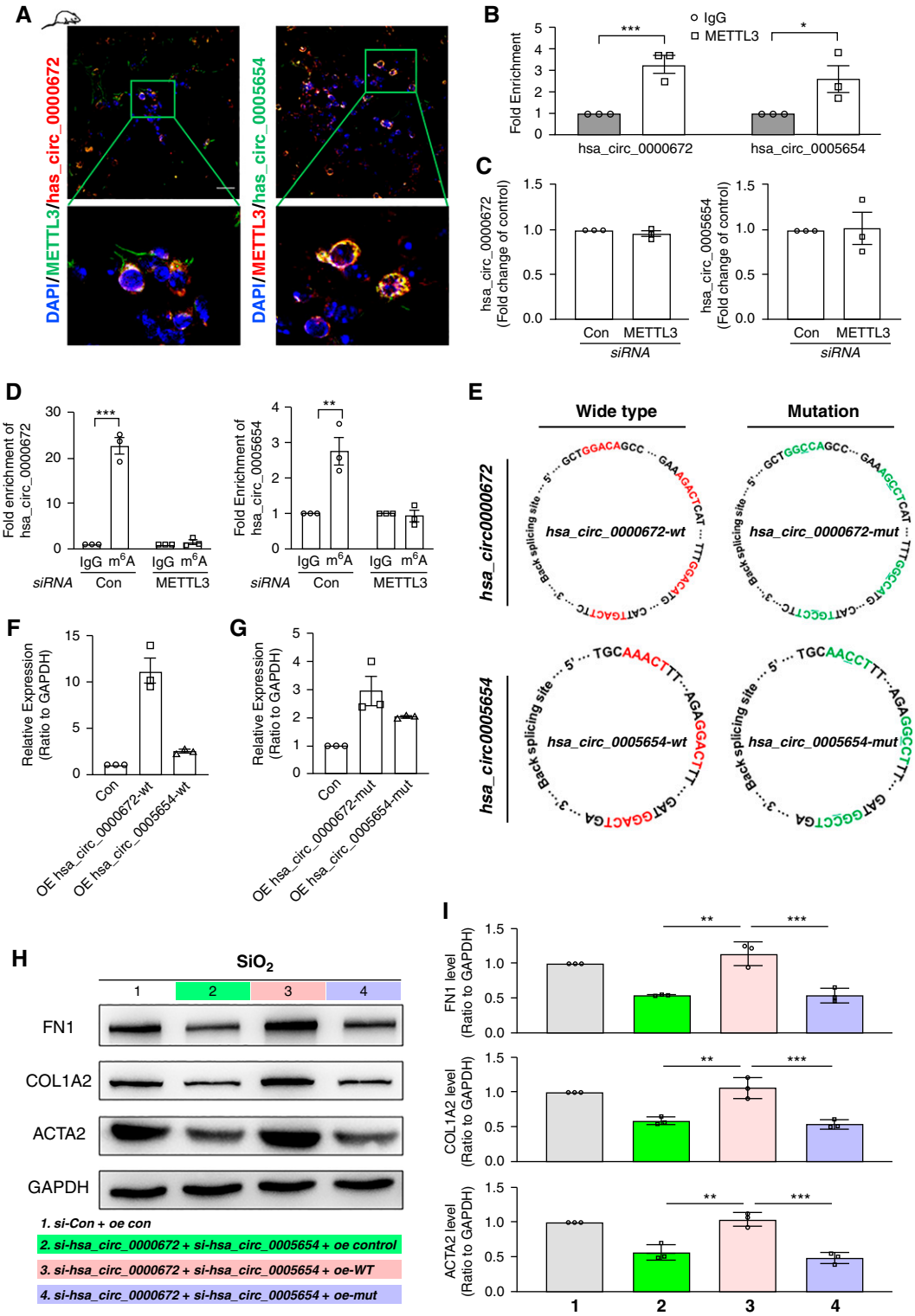

Figure 7. METTL3-mediated circRNA m^{6}A modification promotes the activation of human pulmonary fibroblasts. (*A*) *In situ* hybridization detection of hsa_circ_0000672 and hsa_circ_0005654 colocalization with METTL3. Scale bar, 20 μm. (*B*) RIP test of the interaction of METTL3 with hsa_circ_0000672 and hsa_circ_0005654. The data are presented as the mean ± SD, $n = 3$. *$P < 0.05$ and ***$P < 0.001$. (*C*) Changes in circRNA m^{6}A modification after METTL3 knockdown were detected by me-RIP. The data are presented as mean ± SD, $n = 3$. (*D*) PCR was used to detect the changes in hsa_circ_0000672 and hsa_circ_0005654 expression after knocking down METTL3. The data are presented as the mean ± SD, $n = 3$. **$P < 0.01$ and ***$P < 0.001$. (*E*) Hsa_circ_0000672 and hsa_circ_0005654 with the m^{6}A site–mutated or wild-type overexpression plasmids were constructed. (*F* and *G*) The overexpression efficiency of wild-type and m^{6}A site–mutated overexpression

demonstrate that circRNA m^{6}A modification mediates this inhibition, HPF-a cells were knocked down with hsa_circ_0000672 and hsa_circ_0005654, after which either wild-type or mutant plasmids were transfected into the cells. Transfection of the wild-type plasmid restored the effect of SiO2 on FN1, Collagen 1, and ACTA2 (Figures E10A–E10H). However, transfection of the mutant plasmid attenuated the effects induced by SiO_2 (Figures 7H and 7I), confirming the role of m^{6}A-modified circRNAs in the regulation of SiO_2-induced fibroblast dysfunction.

Discussion

The role of circRNA in various diseases has been recognized, but its mechanism is complex. The current study revealed a new pattern of circRNA action-synergistic effects on circRNA methylation, providing new evidence to explain the precise regulatory mechanism of circRNA in pulmonary fibrosis.

As widely expressed noncoding RNAs, circRNAs are produced by back splicing. Because of their special circular structure, circRNAs are protected from exonuclease cleavage and degradation and thus have high stability (26). CircRNAs have various biological functions. They act as sponges for microRNAs, block mRNA translation, regulate transcription and selective splicing, and interact with RBPs involved in translation (27) and participate in the pathogenesis of glioblastoma, hepatocellular carcinoma, breast cancer, colon cancer, lung cancer, and other cancers (27–29). CircRNA-002178 acts as a competing endogenous RNAs (ceRNA) to promote the expression of PDL1/PD1 in lung adenocarcinoma (30). In gastric cancer, some oncogenic circRNAs promote cell proliferation, migration, and invasion, and some anticancer circRNAs have also been found to be biomarkers for gastric cancer (GC) diagnosis and prognosis (31). In addition, circRNAs regulate energy metabolism in cancer, including glucose metabolism, lipid metabolism, amino acid metabolism, and oxidative respiration (32). The role of circRNA in pulmonary fibrosis was performed recently (33–36). For example, circHECTD1 promotes pulmonary fibrosis via HECTD1-mediated pulmonary fibroblast activation (37) or ZC3H12A-induced macrophage activation (5). Although most of these studies focused on the functional role of a certain circRNA, the current study reveals a novel mode of action of the circRNA-synergistic effect. Because the degree of expression of circRNA in cells is generally low (15), the joint-work mode facilitates subtle control of circRNAs on downstream cascades. The mechanism of circRNA combined effects is complex. One explanation may be the circRNA composition because the clarified circRNAs in the current study have abundant m^{6}A binding sites. Another explanation is the mechanism of action, such as sharing the same downstream target. In the current study, two circRNAs could bind the same protein, eIF4A3. Although two circRNAs have abundant m^{6}A binding sites and the same target protein, cumulative effects may account for the significant effect of the simultaneous knockdown of two circRNAs on fibroblast functions. Another reasonable assumption is that circRNAs with similar characteristics may not only have synergistic effects but also antagonistic or additive action, possibly explaining the subtle regulation of circRNAs. Moreover, knockdown of 000,672 and 0,005,654 circRNAs appears to increase ACTA2 protein concentrations in normal fibroblasts, which may be owing to the nonspecific effect of knockdown because downstream circRNAs are complicated. For example, based upon the ceRNA mechanism, circRNAs may combine with several microRNAs (miRNAs). Another explanation may be that the knockdown of circ000672 and circ0005654 may inhibit the pathological increase in ACTA2, whereas an increase in normal fibroblasts may be a feedback effect.

Epigenetic modification is involved in various biological activities, including DNA methylation, RNA methylation, and histone modification. Recently, an increasing number of studies have been conducted on RNA methylation, in which m^{6}A is the most common type and has been reported to be involved in the occurrence and development of various diseases (29). In hepatoblastoma, m^{6}A-modified mRNAs promote the proliferation of hepatoblastoma by regulating CTNNB1 (38). In the current study, the increase in m^{6}A modification peaked at 2 hours in *in vitro* experiments, indicating a rapid response of SiO_2, which needs to be confirmed by *in vivo* experiments. Recent studies have shown that m^{6}A also occurs in long noncoding RNAs and circRNAs (31, 39). m^{6}A-modified circRNAs have cell type–specific expression, which is different from mRNA expression (40). In addition, m^{6}A modification can regulate circRNA fate, such as regulating the translation of circRNAs, promoting the degradation of circRNAs, and regulating the biogenesis of circRNAs (31, 41, 42). In the current study, high-throughput sequencing of an Arraystar m^{6}A-circRNA epitranscriptomic microarray was applied to detect differences in circRNA m^{6}A modifications. Interestingly, although the microarray results suggested a decrease in most circRNA m^{6}A concentrations and quantities, the m^{6}A concentration of total RNA showed a different pattern. Only a small proportion of circRNAs showed m^{6}A modification patterns similar to those of the total RNA m^{6}A modification. Because of the subtle regulation pattern of circRNAs, these circRNAs, consistent with total RNA, may exhibit a significant effect. Therefore, we selected circRNAs with elevated degrees of m^{6}A modification for subsequent experiments.

The current study suggests that circRNA m^{6}A modification is mainly mediated by METTL3, which may promote fibrosis via fibroblast activation. Previous studies have shown that METTL3-mediated m^{6}A modification is crucial for epithelial-mesenchymal transformation and metastasis in gastric cancer (22). METTL3-mediated m^{6}A modification directly promotes YAP translation and increases YAP activity by regulating the MALAT1-miR-1914–3p-YAP axis, thereby inducing resistance and metastasis in NSCLC (43). Interestingly, we found that METTL3 is elevated at the protein level, but no change is found at the RNA level, indicating that METTL3 may also have modifications, such as posttranslational modifications and

Figure 7. (*Continued*). plasmids in human pulmonary fibroblasts was detected by PCR. The data are presented as the mean ± SD, $n = 3$. (*H* and *I*) WB was conducted to detect the effect of the m^{6}A site–mutated overexpression plasmids on the human pulmonary fibroblast activation markers FN1, Collagen 1 and ACTA2. The data are presented as the mean ± SD, $n = 3$. $^{**}P < 0.01$ and $^{***}P < 0.001$.

posttranscriptional modifications. METTL3 undergoes SUMOylation modification and promotes tumor progression by regulating Snail mRNA homeostasis in hepatocellular carcinoma (44). The detailed mechanism of METTL3 in pulmonary fibrosis deserves further investigation.

Furthermore, METTL3-mediated m^6A-modified hsa_circ_0000672 and hsa_circ_0005654 target eIF4A3, a eukaryotic translation initiation factor involved in circRNA biogenesis. For example, eIF4A3 binds to MMP9 mRNA transcripts, inducing the cyclization of circMMP9 in GBM and increasing the expression of cirMMP9, thereby promoting the proliferation, invasion, and metastasis of GBM cells (45). Interestingly, eIF4A3 mediates the production of circSEPT9, which promotes cell growth and metastasis, thereby promoting the canceration and development of triple-negative breast cancer (46). In addition, has_circ_0030042 regulates abnormal autophagy by targeting eIF4A3 and protecting the stability of atherosclerotic plaques (47). These findings suggest the critical role of eIF4A3 in the biological function of circRNAs. In the current study, eIF4A3, an RBP, interacted wihashsa_circ_000067hasnd hsa_-circ_0005654 to participate in pulmonary fibrosis. However, whether eIF4A3 affects the generation of other circRNAs in pulmonary fibrosis must be clarified.

In conclusion, SiO_2 induces m^6A modifichason of hsa_circ_0000672 and hsa_circ_0005654 via METTL3 in pulmonary fibroblasts; in turn, METTL3 targets eIF4A3 synergistically. eIF4A3 induces proliferation, migration, and activation in pulmonary fibroblasts, followed by pulmonary fibrosis (Figure E11). The synergistic effects may be a considerable pattern of circRNA action, providing a new direction to explore the mechanism of pulmonary fibrosis. ■

Author disclosures are available with the text of this article at www.atsjournals.org.

Acknowledgment: This study is the result of work that was partially supported by the resources and facilities at the core laboratory at the Medical School of Southeast University.

References

1. Leung CC, Yu IT, Chen W. Silicosis. *Lancet* 2012;379:2008–2018.
2. Sato T, Shimosato T, Klinman DM. Silicosis and lung cancer: current perspectives. *Lung Cancer (Auckl)* 2018;9:91–101.
3. Hoy RF, Chambers DC. Silica-related diseases in the modern world. *Allergy* 2020;75:2805–2817.
4. Wang W, Liu HJ, Dai XN, Fang SC, Wang XG, Zhang YM, *et al.* P53/puma expression in human pulmonary fibroblasts mediates cell activation and migration in silicosis. *Sci Rep* 2015;5:16900.
5. Chu H, Wang W, Luo W, Zhang W, Cheng Y, Huang J, *et al.* CircHECTD1 mediates pulmonary fibroblast activation *via* HECTD1. *Ther Adv Chronic Dis* 2019;10:2040622319891558.
6. Salzman J. Circular RNA expression: Its potential regulation and function. *Trends Genet* 2016;32:309–316.
7. Zaccara S, Ries RJ, Jaffrey SR. Reading, writing and erasing mRNA methylation. *Nat Rev Mol Cell Biol* 2019;20:608–624.
8. Zhuang M, Li X, Zhu J, Zhang J, Niu F, Liang F, *et al.* The m6A reader YTHDF1 regulates axon guidance through translational control of Robo3.1 expression. *Nucleic Acids Res* 2019;47:4765–4777.
9. Wang T, Kong S, Tao M, Ju S. The potential role of RNA N6-methyladenosine in cancer progression. *Mol Cancer* 2020;19:88.
10. Lee Y, Choe J, Park OH, Kim YK. Molecular mechanisms driving mRNA degradation by m^6A modification. *Trends Genet* 2020;36:177–188.
11. Lukiw WJ. Circular RNA (circRNA) in Alzheimer's disease (AD). *Front Genet* 2013;4:307.
12. Li XN, Wang ZJ, Ye CX, Zhao BC, Li ZL, Yang Y. RNA sequencing reveals the expression profiles of circRNA and indicates that circDDX17 acts as a tumor suppressor in colorectal cancer. *J Exp Clin Cancer Res* 2018;37:325.
13. Ma HB, Yao YN, Yu JJ, Chen XX, Li HF. Extensive profiling of circular RNAs and the potential regulatory role of circRNA-000284 in cell proliferation and invasion of cervical cancer via sponging miR-506. *Am J Transl Res* 2018;10:592–604.
14. Zhang Y, Du L, Bai Y, Han B, He C, Gong L, *et al.* CircDYM ameliorates depressive-like behavior by targeting miR-9 to regulate microglial activation via HSP90 ubiquitination. *Mol Psychiatry* 2020;25:1175–1190.
15. Chen L, Luo W, Zhang W, Chu H, Wang J, Dai X, *et al.* circDLPAG4/HECTD1 mediates ischaemia/reperfusion injury in endothelial cells via ER stress. *RNA Biol* 2020;17:240–253.
16. Zhou B, Yu JW. A novel identified circular RNA, circRNA_010567, promotes myocardial fibrosis via suppressing miR-141 by targeting TGF-β1. *Biochem Biophys Res Commun* 2017;487:769–775.
17. Xu J, Wan Z, Tang M, Lin Z, Jiang S, Ji L, *et al.* N^6-methyladenosine-modified CircRNA-SORE sustains sorafenib resistance in hepatocellular carcinoma by regulating β-catenin signaling. *Mol Cancer* 2020;19:163.
18. Jiang R, Han L, Gao QQ, Chao J. ZC3H4 mediates silica-induced endoMT via ER stress and autophagy. *Environ Toxicol Pharmacol* 2021;84:103605.
19. Jiang R, Zhou Z, Liao Y, Yang F, Cheng Y, Huang J, *et al.* The emerging roles of a novel CCCH-type zinc finger protein, ZC3H4, in silica-induced epithelial to mesenchymal transition. *Toxicol Lett* 2019;307:26–40.
20. Fang S, Guo H, Cheng Y, Zhou Z, Zhang W, Han B, *et al.* circHECTD1 promotes the silica-induced pulmonary endothelial-mesenchymal transition via HECTD1. *Cell Death Dis* 2018;9:396.
21. Li X, Yang L, Chen LL. The biogenesis, functions, and challenges of circular RNAs. *Mol Cell* 2018;71:428–442.
22. Yue B, Song C, Yang L, Cui R, Cheng X, Zhang Z, *et al.* METTL3-mediated N6-methyladenosine modification is critical for epithelial-mesenchymal transition and metastasis of gastric cancer. *Mol Cancer* 2019;18:142.
23. Al-Juboori SI, Vadakekolathu J, Idri S, Wagner S, Zafeiris D, Pearson JR, *et al.* PYK2 promotes HER2-positive breast cancer invasion. *J Exp Clin Cancer Res* 2019;38:210.
24. Naser R, Aldehaiman A, Díaz-Galicia E, Arold ST. Endogenous control mechanisms of FAK and PYK2 and their relevance to cancer development. *Cancers (Basel)* 2018;10:196.
25. Li F, Kennedy S, Hajian T, Gibson E, Seitova A, Xu C, *et al.* A radioactivity-based assay for screening human m6A-RNA methyltransferase, METTL3-METTL14 complex, and demethylase ALKBH5. *J Biomol Screen* 2016;21:290–297.
26. Kristensen LS, Andersen MS, Stagsted LVW, Ebbesen KK, Hansen TB, Kjems J. The biogenesis, biology and characterization of circular RNAs. *Nat Rev Genet* 2019;20:675–691.
27. Han B, Chao J, Yao H. Circular RNA and its mechanisms in disease: From the bench to the clinic. *Pharmacol Ther* 2018;187:31–44.
28. Lei M, Zheng G, Ning Q, Zheng J, Dong D. Translation and functional roles of circular RNAs in human cancer. *Mol Cancer* 2020;19:30.
29. Zeng K, Chen X, Xu M, Liu X, Hu X, Xu T, *et al.* CircHIPK3 promotes colorectal cancer growth and metastasis by sponging miR-7. *Cell Death Dis* 2018;9:417.
30. Wang J, Zhao X, Wang Y, Ren F, Sun D, Yan Y, *et al.* CircRNA-002178 act as a ceRNA to promote PDL1/PD1 expression in lung adenocarcinoma. *Cell Death Dis* 2020;11:32.
31. Li R, Jiang J, Shi H, Qian H, Zhang X, Xu W. CircRNA: a rising star in gastric cancer. *Cell Mol Life Sci* 2020;77:1661–1680.
32. Yu T, Wang Y, Fan Y, Fang N, Wang T, Xu T, *et al.* CircRNAs in cancer metabolism: a review. *J Hematol Oncol* 2019;12:90.

33. Li C, Wang Z, Zhang J, Zhao X, Xu P, Liu X, *et al.* Crosstalk of mRNA, miRNA, lncRNA, and circRNA and their regulatory pattern in pulmonary fibrosis. *Mol Ther Nucleic Acids* 2019;18:204–218.
34. Dai X, Cheng Y, Wang C, Huang J, Chao J. Role of circular RNAs in visceral organ fibrosis. *Food Chem Toxicol* 2021;150:112074.
35. Zhang JX, Lu J, Xie H, Wang DP, Ni HE, Zhu Y, *et al.* circHIPK3 regulates lung fibroblast-to-myofibroblast transition by functioning as a competing endogenous RNA. *Cell Death Dis* 2019;10:182.
36. Li J, Li P, Zhang G, Qin P, Zhang D, Zhao W. CircRNA TADA2A relieves idiopathic pulmonary fibrosis by inhibiting proliferation and activation of fibroblasts. *Cell Death Dis* 2020;11:553.
37. Zhou Z, Jiang R, Yang X, Guo H, Fang S, Zhang Y, *et al.* CircRNA mediates silica-induced macrophage activation via HECTD1/ZC3H12A-dependent ubiquitination. *Theranostics* 2018;8:575–592.
38. Liu L, Wang J, Sun G, Wu Q, Ma J, Zhang X, *et al.* m^6A mRNA methylation regulates CTNNB1 to promote the proliferation of hepatoblastoma. *Mol Cancer* 2019;18:188.
39. Ni W, Yao S, Zhou Y, Liu Y, Huang P, Zhou A, *et al.* Long noncoding RNA GAS5 inhibits progression of colorectal cancer by interacting with and triggering YAP phosphorylation and degradation and is negatively regulated by the m^6A reader YTHDF3. *Mol Cancer* 2019; 18:143.
40. Zhou C, Molinie B, Daneshvar K, Pondick JV, Wang J, Van Wittenberghe N, *et al.* Genome-wide maps of m6A circRNAs identify widespread and cell-type-specific methylation patterns that are distinct from mRNAs. *Cell Rep* 2017;20:2262–2276.
41. Chen RX, Chen X, Xia LP, Zhang JX, Pan ZZ, Ma XD, *et al.* N^6-methyladenosine modification of circNSUN2 facilitates cytoplasmic export and stabilizes HMGA2 to promote colorectal liver metastasis. *Nat Commun* 2019;10:4695.
42. Yang Y, Fan X, Mao M, Song X, Wu P, Zhang Y, *et al.* Extensive translation of circular RNAs driven by N^6-methyladenosine. *Cell Res* 2017;27:626–641.
43. Jin D, Guo J, Wu Y, Du J, Yang L, Wang X, *et al.* m^6A mRNA methylation initiated by METTL3 directly promotes YAP translation and increases YAP activity by regulating the MALAT1-miR-1914-3p-YAP axis to induce NSCLC drug resistance and metastasis. *J Hematol Oncol* 2019;12:135.
44. Xu H, Wang H, Zhao W, Fu S, Li Y, Ni W, *et al.* SUMO1 modification of methyltransferase-like 3 promotes tumor progression via regulating Snail mRNA homeostasis in hepatocellular carcinoma. *Theranostics* 2020;10:5671–5686.
45. Wang R, Zhang S, Chen X, Li N, Li J, Jia R, *et al.* EIF4A3-induced circular RNA MMP9 (circMMP9) acts as a sponge of miR-124 and promotes glioblastoma multiforme cell tumorigenesis. *Mol Cancer* 2018;17:166.
46. Zheng X, Huang M, Xing L, Yang R, Wang X, Jiang R, *et al.* The circRNA circSEPT9 mediated by E2F1 and EIF4A3 facilitates the carcinogenesis and development of triple-negative breast cancer. *Mol Cancer* 2020;19:73.
47. Yu F, Zhang Y, Wang Z, Gong W, Zhang C. Hsa_circ_0030042 regulates abnormal autophagy and protects atherosclerotic plaque stability by targeting eIF4A3. *Theranostics* 2021;11: 5404–5417.